water

MDPI

Article

Hydrological Risk Analysis of Dams: The Influence of Initial Reservoir Level Conditions

Ivan Gabriel-Martin *, Alvaro Sordo-Ward, Luis Garrote and Isabel Granados

Department of Civil Engineering: Hydraulics, Energy and Environment, Universidad Politécnica de Madrid, 28040 Madrid, Spain; alvaro.sordo.ward@upm.es (A.S.-W.); l.garrote@upm.es (L.G.); i.granados@upm.es (I.G.)

* Correspondence: i.gabriel@upm.es; Tel.: +34-913-366703

Received: 31 December 2018; Accepted: 27 February 2019; Published: 5 March 2019

Abstract: In this paper, we present a method to assess the influence of the initial reservoir level in hydrological dam safety and risk analysis. Traditionally, in professional practice, the procedures applied are basically deterministic. Several physical processes are defined deterministically, according to the criteria of the designer (usually in the conservative side), although there is a high degree of uncertainty regarding these processes. A relevant variable is the reservoir level considered at the beginning of flood events. Hydrological dam safety assessment methods traditionally assume that the reservoir is initially full when it receives the design flood, thus, staying in the conservative side when designing a new dam. However, the distribution of reservoir levels at the beginning of flood episodes takes more importance for evaluating the real risk for the dams in operation. We analyzed three different scenarios—initial reservoir level equal to maximum normal level, equal to a maximum conservation level, and following the probability distribution from the historical records. To do so, we presented a method applied to a gated-spillway dam located in the Tagus river basin. A set of 100,000 inflow hydrographs was generated through a Monte Carlo procedure, by reproducing the statistics of the main observed hydrograph characteristics—peak flow, volume, and duration. The set of 100,000 hydrographs was routed through the reservoir applying the Volumetric Evaluation Method as a flood control strategy. In order to compare the three scenarios, we applied an economic global risk index. The index combines the hydrological risk for the dam, linked to the maximum water level reached in the reservoir, during the flood routing, and the flood risk in the downstream river reach, linked to the discharge releases from the dam. The results showed the importance of accounting for the fluctuation of initial reservoir levels, for assessing the risk related to hydrological dam safety. Furthermore, a procedure to quantify the uncertainty associated with the effects of initial reservoir level on hydrological dam safety, has been proposed.

Keywords: dam; initial reservoir level; hydrological dam safety; downstream safety; global risk index; stochastic approach

1. Introduction

Failure of large dams is a concern in many countries, due to the high economic and social consequences associated with it. When designing a dam, engineers usually apply techniques to assure that the risk of dam failure is low, but the standards are applied differently, depending on the country in which the dam is located [1]. Even though the risk is low, the associated risk should be recalculated, as the legal regulations, climate conditions, basin, and dam characteristics may vary with time [2].

The field of dam risk assessment has evolved, worldwide, with the appearance of different guides and procedures in several countries [3–5], to support dam stake-holders in the decision-making process related to dam safety. It is also well-known that, due to the high variability of the natural processes, the assessment of dam safety introduces uncertainties that should be assessed as a part of the process. However, analyzing this uncertainty is a complex task [6–8].

Moreover, human actions also provide additional sources of uncertainty to the analysis. By the use of probabilistic approaches, variability of the variables involved can be assessed [9–13]. One such variable related to human actions is the variability of the initial reservoir level, due to its connection to the operation of reservoirs. As stated by different authors [14–17], this variable should be assessed to obtain more realistic results, when it comes to the analysis of hydrological dam and downstream safety. Carvajal et al. [14] studied three real dams, with different levels of reservoir fluctuation and spillways, whereas Aranda Domingo [15] and Gabriel-Martin et al. [16,17] studied one irrigation dam each. All concluded that accounting for reservoir levels fluctuations is desirable, moreover, when the dam is operated on a seasonal basis as reservoirs, its main purpose is irrigation, regardless of the spillway and dam typology.

Within this study, we proposed a methodology to economically analyze the affection of the initial reservoir level, in hydrological dams and downstream safety, by the application of economic risk indices [6,18]. Furthermore, the uncertainty associated with the initial variable level has been studied through a novel approach, for the case study. First, a stochastic procedure has been presented. Then, we applied this methodology to a dam configuration based on a real case study. Finally, we analyzed and discussed the results obtained, highlighting the main conclusions of this study.

2. Materials and Methods

A probabilistic approach was implemented (Figure 1), based on a Monte Carlo approach (dotted points in Figure 1). The process was as follows:

- Generation of synthetic inflow hydrographs: An ensemble of synthetic inflow hydrographs representative of the observed historical annual maximum floods was generated.
- Stochastic initial reservoir level assignment: Depending on the scenario studied (a total of three, as explained in Section 2.2), an initial reservoir level was assigned to each inflow hydrograph. Furthermore, an uncertainty analysis of the variable initial reservoir level (Scenario 3) was carried out.
- Reservoir-Dam flood operation: For each analyzed scenario (a total of three), the ensemble of hydrographs was routed through the reservoir, obtaining a set of maximum reservoir levels and maximum outflows.
- Risk-Index analysis: By using a global risk index analysis [6,18], we compared all the scenarios studied.

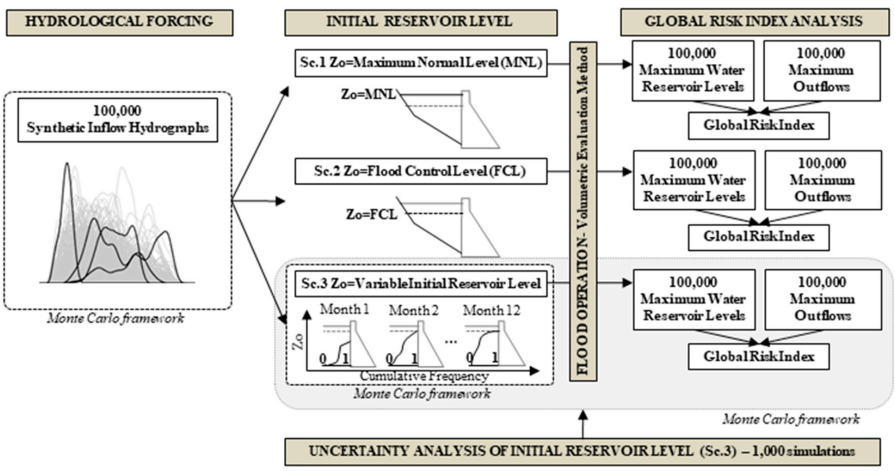

Figure 1. General scheme of the methodological approach. Sc. 1, Sc. 2, and Sc. 3 stand for the three different scenarios of initial reservoir level (Zo) studied.

2.1. Generation of Synthetic Reservoir Inflow Hydrographs

In several countries, regulations require consideration of return periods of up to 10,000 years [1]. To assure that the results obtained were representative, a set of 100,000 hydrographs was generated [19–22], by applying a methodology previously presented by Gabriel–Martin et al. [16]. This methodology permitted the obtainment of stochastic inflow hydrographs, representative of the observed annual floods. The methodology can be summed up as follows (cf. Gabriel–Martin et al. [16]):

1. Generation of 100,000 flood event durations, following the empirical probability distribution of historical floods.
2. For each element of the 100,000 generated durations, the respective hydrograph volume was obtained, following the statistic distribution of the associated duration within a Monte Carlo framework.
3. Each flood volume value was converted to a cumulated rainfall depth, divided by the basin area, and a runoff-rainfall conversion was applied on the basis of the Curve Number method [23].
4. Each cumulated rainfall depth was distributed temporally by applying a second order autoregressive second order moving average (ARMA (2,2)) model [22].
5. Applying the Curve Number method [23] and the Soil Conservation Service dimensionless unit hydrograph procedure [23], 100,000 hydrographs were generated, which followed the empirical probability distributions of volume and duration.

2.2. Initial Reservoir Level Scenarios and Uncertainty Analysis

In order to assess the influence of initial reservoir levels, we studied three different scenarios:

- Scenario 1 (Sc. 1): For all 100,000 hydrographs, the initial reservoir level was set equal to the Maximum Normal Level (MNL). MNL is a constant level, and refers to the maximum acceptable level in the reservoir, under ordinary operation. This reservoir level was set in the design phase of the dam.
- Scenario 2 (Sc. 2): For all 100,000 hydrographs, initial reservoir level was set equal to the Flood Control Level (FCL). FCL is the level which cannot be overpassed under ordinary operation of the reservoir (prior to a flood event), assuring that the design flood does not compromise the hydrological dam safety. We defined this level as the initial reservoir level that, after routing the set of 100,000 synthetic flood events through the reservoir, which resulted in a maximum water reservoir level with a return period of 1000 years ($MWRL_{TR = 1000y}$), which was equal to the Design Flood Level (DFL), fulfilling the regulation standards. FCL is always lower or equal to the MNL, as it is usually defined to fulfill the regulation standards that are set in the years after the construction of the dam.
- Scenario 3 (Sc. 3): First, following Gabriel-Martin et al. [16] we associated each one of the 100,000 hydrographs to a month of occurrence, using the empirical distribution of months of occurrence of historical annual maximum floods. Then, for each one of the 100,000 hydrographs, a variable initial reservoir level was assigned. To do so, we first analyzed daily reservoir level measurements in the reservoir. We removed the period of filling-up of the reservoir, as it did not represent the normal operation of the reservoir [5]. Then, we obtained the empirical monthly distribution of the historical reservoir levels. Using this distribution, we generated a set of 100,000 initial reservoir levels, each one associated with each month, in the aforementioned series of 100,000 months, and, consequently, to each one of the 100,000 inflow hydrographs.

Finally, in order to assess the uncertainty associated with the initial reservoir level, we carried out a set of 1000 simulations of Sc.3, within a Monte Carlo framework (Figure 1). This way, we were able to evaluate how the variability of this variable affected the hydrological dam and downstream safety.

2.3. Reservoir-Dam Flood Operation

For each generated hydrograph (100,000 incoming floods) and scenario, we simulated the operation of the dam gates applying the Volumetric Evaluation Method (VEM) [6,24,25]. VEM is a real-time flood control method usually applied in Spanish dams. This method is based on four principles:

- Outflows are lower than or equal to the maximum antecedent inflows.
- Outflows increase when inflows increase.
- The higher the reservoir level, the higher the percentage of outflow increase.
- If the reservoir is at maximum capacity, outflows are equal to inflows while gates are partially opened.

The released outflow at each operation hour (time step) was the minimum among: (a) the outflows proposed by VEM, (b) the maximum discharge capacity at the current reservoir level, and (c) the maximum of the antecedent inflows. Once the gates were completely opened, the spillway structure behaved as a fixed-crest spillway. The initial reservoir level depended on the scenario studied. After applying the VEM to all scenarios, we obtained the following results for each scenario:

- Scenario 1 and Scenario 2: For each scenario we obtained a set of 100,000 reservoir level and 100,000 outflow flood control time series, from which we derived the Maximum Water Reservoir Levels (MWRL) and Maximum Outflows (MO) frequency curves.
- Scenario 3: In this scenario, due to the uncertainty assessment, we obtained a set of 1000 MWRL and MO frequency curves, derived from 1000 sets of 100,000 reservoir level and outflow time series.

2.4. Risk Index Analysis

To carry out an economic assessment of the obtained results, we implemented the global risk index (I_R) analysis proposed by Bianucci et al. [18]. This method accounts for a single indicator of the global risk associated with the MWRL and MO. To do so, it relies on the concept of expected annual damage (EAD) [26]. EAD is frequently used for quantifying the damage associated with floods [18]. It represents the area under the damage-probability curve, which is calculated as follows (Equation (1)):

$$\mathrm{EAD} = \sum_{i=1}^{M-1} (p_i - p_{i+1}) \cdot \frac{(D_i + D_{i+1})}{2}, \quad (1)$$

where M represents the number of points of probability-damage considered in the curve, p represents the exceedance probability and D is the associated damage. We applied the EAD concept to obtain two different indices—one related to the failure of the dam due to overtopping (I_F), and the second one associated with the damage (without dam failure) caused by the resulting outflows from the dam flood control operation (I_{NF}). Once the two indices were obtained, we calculated the global risk index (I_R) as the aggregation of both indices [6,18] (Equation (2)):

$$I_R = I_F + I_{NF}, \quad (2)$$

where I_F, I_{NF}, and I_R are expressed in euros. To obtain both I_F and I_{NF}, we applied Equations (3) and (4) respectively:

$$I_F = \sum_{i=1}^{N-1} (p(\mathrm{MWRL}_i) - p(\mathrm{MWRL}_{i+1})) \cdot \left(D_{\mathrm{MWRL}} \left(\frac{\mathrm{MWRL}_i + \mathrm{MWRL}_{i+1}}{2} \right) \right), \quad (3)$$

$$I_{NF} = \sum_{i=1}^{N-1} (p(\mathrm{MO}_i) - p(\mathrm{MO}_{i+1})) \cdot \left(D_{\mathrm{MO}} \left(\frac{\mathrm{MO}_i + \mathrm{MO}_{i+1}}{2} \right) \right), \quad (4)$$

where D_{MWRL} and D_{MO} are the damage functions (expressed in euros) for failure and non-failure respectively, the index i represents the position of the sorted series (ascending order up to N, which is equal to 100,000 in the current study) of MWRLs and MOs and p represents the exceedance probability.

Therefore, to apply the global risk index methodology, it is necessary to obtain the damage cost curves (D_{MWRL} and D_{MO}). To do so, we proceeded as follows:

1. Damage cost curve associated with overtopping dam failure: It is important to highlight the difference between the risk of damage associated with MOs and MWRLs. While in the case of MOs, there is an actual damage associated with a determined flow, reaching a certain MWRL might not have a damage associated [18]. Thus, reaching a certain reservoir level does not have to result into the dam failing, but there is a risk of failing. Therefore, following the approach proposed by Bianucci et al. [18], we calculated the damage cost curve as (Equation (5)):

$$D_{MWRL}(MWRL_i) = p(break\,|\,MWRL_i) \cdot Cost_{break}, \tag{5}$$

   where $Cost_{break}$ represents the damage cost if the dam fails (expressed in euros), whereas $p(break\,|\,MWRL_i)$ is the probability of overtopping failure conditioned to reaching a certain level in the reservoir ($MWRL_i$). $Cost_{break}$ was estimated as the cost of reconstruction of the dam aggregated to the estimated downstream damage, when overtopping failure occurred. We considered $Cost_{break}$ as a constant value, as we only had data of the estimated downstream damage associated with the flood wave caused by the overtopping failure mode, accounted by the Dam Master Plan (failure when reservoir level is at Crest of Dam (COD)). The $p(break\,|\,MWRL_i)$, according to Bianucci et al. [18] can be represented as the probability of reaching the reservoir level at COD, once $MWRL_i$ has been reached during a flood event (Equation (6)):

$$p(break|MWRL_i) = p(MWRL_{MAX} \geq COD|MWRL_i) = \frac{n\ events\ MWRL_{MAX} \geq COD}{n\ events\ MWRL_{MAX} \geq MWRL_i} \tag{6}$$

   This expression was estimated by routing 100,000 synthetic floods (applying the methodology shown in Section 2.1), with a moderate to extreme return period of peak-flow (10 to 200,000 years). By assuming that overtopping leads to dam failure, p $(break\,|\,MWRL_i)$ was calculated as the number of events in which $MWRL_{MAX} \geq COD$, over the number of events in which $MWRL_{MAX} \geq MWRL_i$.
2. Damage cost curves associated with non-failure: Regarding D_{MO} was estimated that by analyzing the possible damages downstream, based on the information included in the Spanish National GIS viewer about flood risk assessments through flood plain analysis [27].

2.5. Limitations of the Methodology

The methodology applied had some limitations that should be noted:

1. Regarding the inflow hydrographs, the limitations of the methodology were those discussed in [16]: The assumption that the maximum annual flood event corresponded to the maximum annual peak-flow, the independence in the distribution fitting of maximum annual volumes, and not considering the snowmelt in the hydrological model. Furthermore, we generated the synthetic hydrographs by using a sample of 55 years of observed local data. It is important to point out that, if possible, paleo flood data or regionalization techniques should be used to improve the accuracy of the method [5].
2. Regarding the flood control operation method (VEM), it has the advantage of simplicity. However, it lacks the flexibility of being adapted to the specific characteristics of the dam, other than the flood control volume. Other flood control management models could have been tested, for instance the K-Method [6].

3. Regarding the risk index analysis, we assumed a constant value of $Cost_{break}$. According to the available data, we did not consider the dependence of the water height and volume in the reservoir on the downstream floods. In this case, the $Cost_{break}$ could be defined as a function of MWRLs. The reader is referred to [2,5,28] for further details on this approach. Furthermore, there also existed uncertainties with the estimation of downstream damages (for example, the uncertainties associated with hydraulic calculations of the inundation zone in the event of a dam failure).
4. The methodology was applied to one dam with a specific configuration, which can limit the extrapolation of the results obtained within this study. For instance, results related to the initial reservoir level could vary if there were modifications in the regular operation of the reservoir and seasonal variations in the flood control levels were accounted (cf. [14,16,17]). Furthermore, possibility of gate failure was not considered [16].

2.6. Case Study

The proposed methodology was applied in a case study, based on a gated-spillway gravity dam located in the Tagus river basin. The dam was located in Western Spain (province of Caceres). The dam watershed has an extension of 1850 km^2. The climate within the area of the study was Continental, with a mean annual precipitation of 1000 mm and a mean annual runoff value of 1020 hm^3. The main purpose of the reservoir was irrigation.

Table 1 shows the main characteristics of the dam and its reservoir. The dam's main spillway consisted of five Tainter gates, which were ten meters wide by 5.75 m high, each. The other operative discharge structure considered was a bottom outlet in the dam body.

Table 1. Characteristic reservoir levels (in meters above sea level (m.a.s.l.)) and spillway of the dam configuration studied.

Reservoir Levels (m.a.s.l.)		**Maximum Outflow Capacity at Maximum Normal Level (MNL) (m^3/s)**	
Gated spillway crest	380.25	Gated-spillway	2200
Maximum Normal Level (MNL)	386		
Design flood level (DFL)	387	Bottom outlet	57
Crest of dam (COD)	388		

To carry out the study, we used a gauge station located at the dam location, with the available data on the daily inflows and reservoir volumes from 1958/1959 to 2012/2013 (hydrological years, from 1 October to 30 September). With these data, we were able to generate the synthetic inflow hydrographs and obtain the statistic distributions of the initial reservoir levels for Sc. 3.

3. Results and Discussion

3.1. Generation of Synthetic Reservoir Inflow Hydrographs

We generated 100,000 reservoir inflow hydrographs, stochastically, using the available 55 years of daily reservoir inflow data (1958/59–2012/13). First, as exposed in the methodology, we obtained the empirical probability distribution of maximum annual flood durations. The durations were within the range of three to nine days, the most frequent values being five and six days (comprising 47.3% of the observed values). With a Monte Carlo procedure, we generated a set of 100,000 hydrograph durations (Figure 2a).

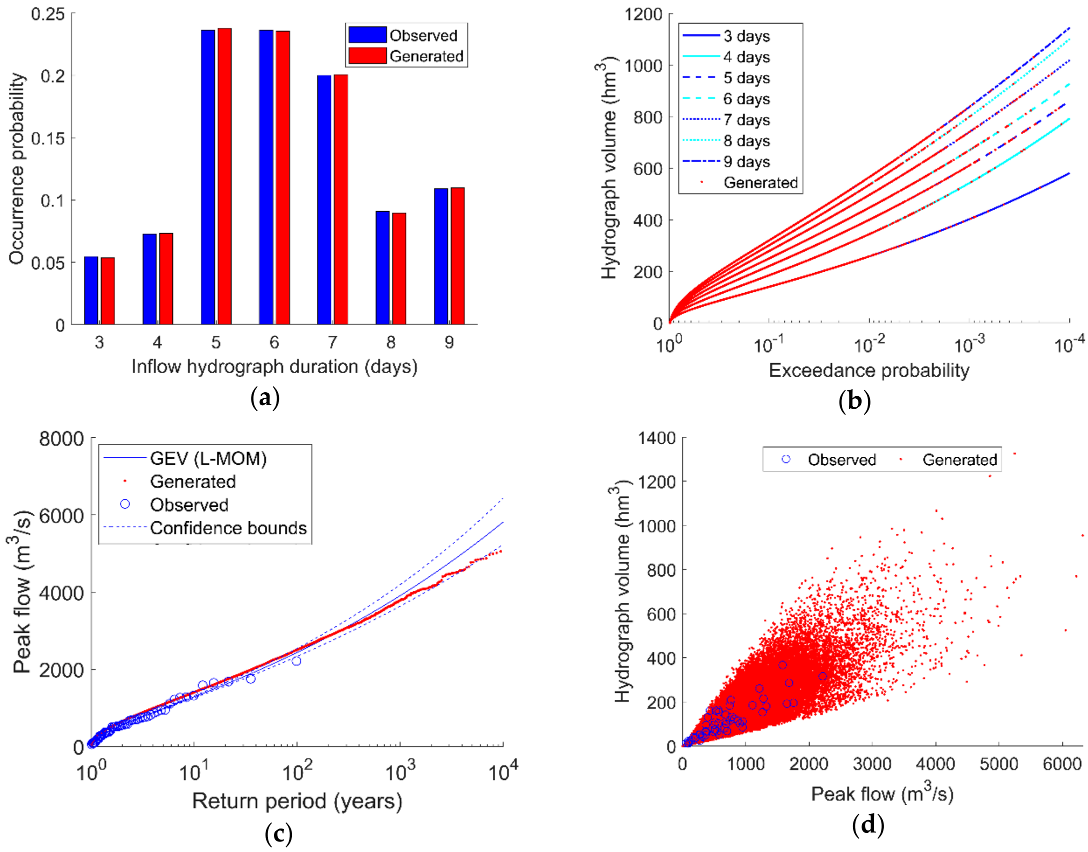

Figure 2. Synthetic inflow hydrograph generation. (**a**) Frequency distribution of the observed (blue) and simulated (red) reservoir inflow hydrograph duration (**b**) Generalized Extreme Value (GEV) distribution fits using the L-Moments (L-MOM) technique of maximum annual hydrograph volume for the different observed durations (blue lines) and the simulated volumes (red dots). (**c**) GEV fits using the L-Moments (L-MOM) technique of the maximum annual instantaneous peak flows. Blue circles represent the maximum annual instantaneous peak flow with return periods obtained by applying the Gringorten plotting position formula, blue continuous line represents the GEV L-MOM fit, blue dashed lines represent the 99% confidence bounds, whereas the red dots represent the maximum peak flows generated with a return period obtained by applying the Gringorten plotting position formula. (**d**) Sample of 100,000 simulated floods (red dots) plotted with the observed floods (blue-edged circles).

We calculated the volume frequency curves (VFCs), each one associated with one duration (from three to nine days). We fitted them to a Generalized Extreme Value (GEV) distribution, with the estimated parameters, using the L-Moments technique [29]. All fitted statistic distributions passed the Kolmogorov–Smirnov goodness of fit test. Figure 2b shows the fits (*p*-Values were within the range of 0.997 to 0.999, for all durations). Then, we generated the 100,000 hydrographs as exposed in the methodology. To assure the validity of the sample generated, we obtained the synthetic peak flow frequency curve (PFFC), in order to compare it with the synthetic generated one (at an hourly time step). We estimated the instantaneous observed peak flows, using the equation recommended in the literature for the Tagus river basin area [28] (Equation (7)):

$$\mathrm{IMF} = \mathrm{MDF}\cdot\left(1 + 5.01\cdot\mathrm{A}^{-0.38}\right), \tag{7}$$

where IMF and MDF are the instantaneous maximum flow and the maximum annual mean daily flow respectively (m^3/s) and A is the watershed area in km^2 [27]. We also fitted the pseudo-observed instantaneous PFFC to a GEV distribution using L-Moments technique [29], which also passed Kolmogorov–Smirnov goodness of fit test with a *p*-Value of 0.997. Then, by using the Gringorten plotting position formula [30], we compared the 100,000 peak flows (synthetic PFFC) of the sample generated with the pseudo-observed PFFC (Figure 2c). Finally, Figure 2d shows the peak flow volume relationship between the observed and the generated sample, showing how the synthetic events properly represent the main hydrograph characteristics.

3.2. Initial Reservoir Level Assesment

In order to assess the initial reservoir level, we carried out an analysis of the observed data:

1. First, we analyzed in which months the annual maximum mean daily flow occurred (from the hydrological year of 1958/1959 to 2012/2013) and obtained the probability distribution of occurrence of the monthly annual floods (Figure 3a).
2. Then, we analyzed the daily reservoir volumes to obtain the initial reservoir volume frequency distributions. We discarded the reservoir data from 1958/1959 to 1965/1966, as, in those years, the reservoir was filling-up and did not represent the normal operation years. We also checked that no significant changes in the reservoir operation strategy had happened during the analyzed period (1966/1967 to 2012/2013). To do so, we calculated the cumulative monthly supply, cumulative monthly storage, and cumulative monthly ratio of supply over storage (Figure 3b, from left to right). It is shown that the relations are almost linear, being the small variations due to the natural variability of inflows.
3. Finally, we obtained the cumulative frequency distribution of exceedance of the monthly daily reservoir levels, using the reservoir level time series from 1966/1967 to 2012/2013 (Figure 3c).

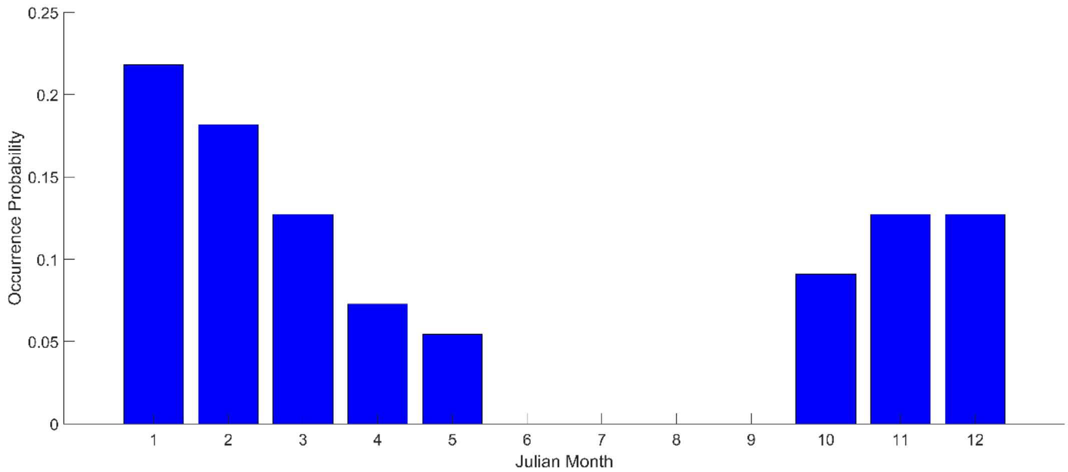

(**a**)

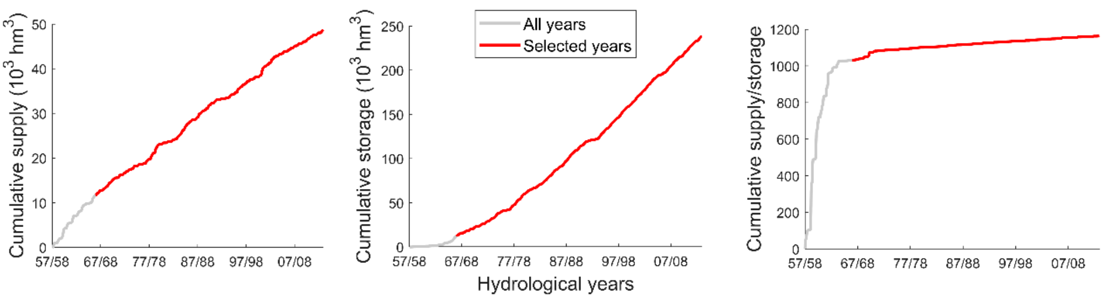

(**b**)

Figure 3. *Cont.*

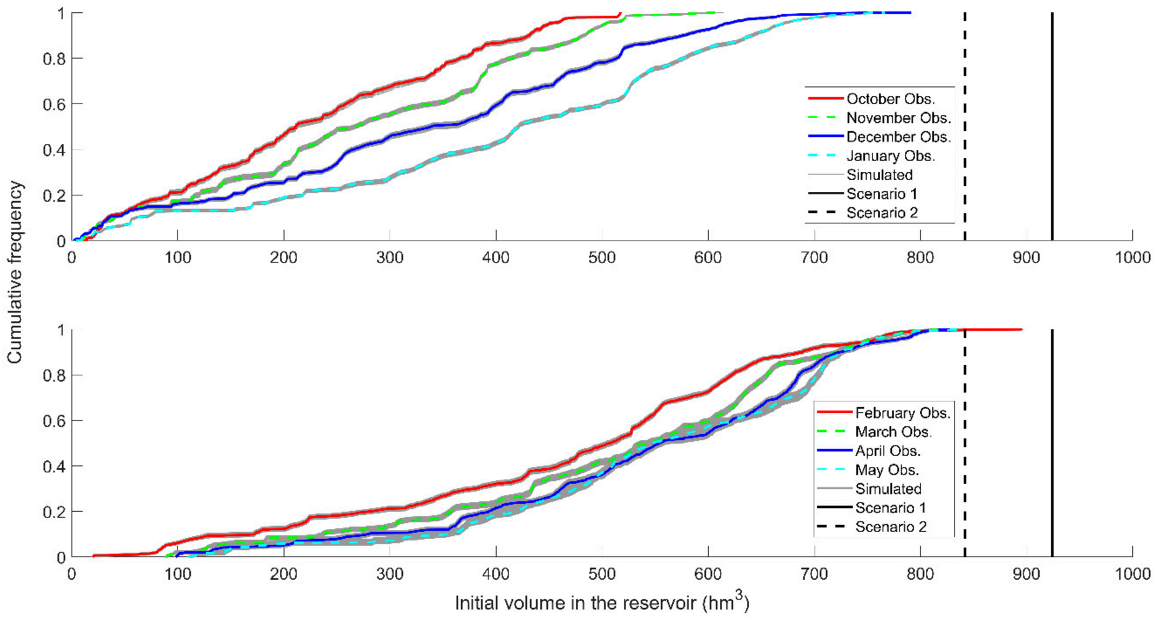

(**c**)

Figure 3. Initial reservoir level assessment. (**a**) Occurrence probability of monthly maximum annual flood. (**b**) Cumulative monthly supply, storage, and supply over storage values. The whole period is represented in grey (1958/1959 to 2012/2013), whereas the selected period is represented in red (1966/1967 to 2012/2013). (**c**) Empirical monthly reservoir level distributions associated with each month in (**a**). Different color lines (red, green, blue, and cyan) represent the observed (Obs.) reservoir level distribution. Grey lines represent the 1000 simulations of monthly initial reservoir levels distributions for Scenario 3. Scenario 1 is represented in a black continuous line, whereas Scenario 2 is represented in a dashed black line.

As exposed in the methodology, we analyzed three different scenarios:

- Scenario 1: For all the 100,000 hydrographs, the initial reservoir level was set at MNL (386 m above sea level (m.a.s.l.)) and corresponded to a volume in the reservoir of 924 hm^3 (vertical black continuous line, in Figure 3c).
- Scenario 2: For all the 100,000 hydrographs, the initial reservoir level was set at FCL (384 m.a.s.l.) and corresponded to a volume in the reservoir of 841.9 hm^3 (black vertical dashed line in Figure 3c). As exposed in the methodology, we calculated this initial reservoir level as the one that resulted in $\text{MWRL}_{\text{TR = 1000y}}$ = DFL.
- Scenario 3. For each one of the 100,000 hydrographs, a variable initial reservoir level was assigned within a Monte Carlo framework and a set of 100,000 initial reservoir levels were generated. We repeated this procedure 1000 times to obtain 1000 frequency distributions of monthly initial reservoir volumes (in red in Figure 3c).

In Figure 3c, it can be seen that the annual fluctuation of the reservoir is reflected in the cumulative probability frequency curves. The reservoir presented the lowest levels in October (discarding from June to September, months in which no floods were registered), due to the end of irrigation season. This operation policy might be of importance when analyzing the influence of the initial reservoir level, as pointed by Gabriel–Martin et al. [16] and Carvajal et al. [14].

3.3. Maximum Water Reservoir Level and Maximum Outflow Frequency Curves

As exposed in the methodology, we obtained 100,000 MWRLs and 100,000 MOs for Sc. 1 (red in Figure 4) and Sc. 2 (green lines in Figure 4), whereas we obtained 1000 sets (to analyze uncertainty related to the initial variable reservoir level) of 100,000 MWRLs and 100,000 MOs for Sc. 3 (each one of the 1000 sets is represented in grey, within Figure 4, whereas the mean of the 100,000 simulations is represented in a blue continuous line and the 2.5% and 97.5% percentiles are represented in blue dashed lines).

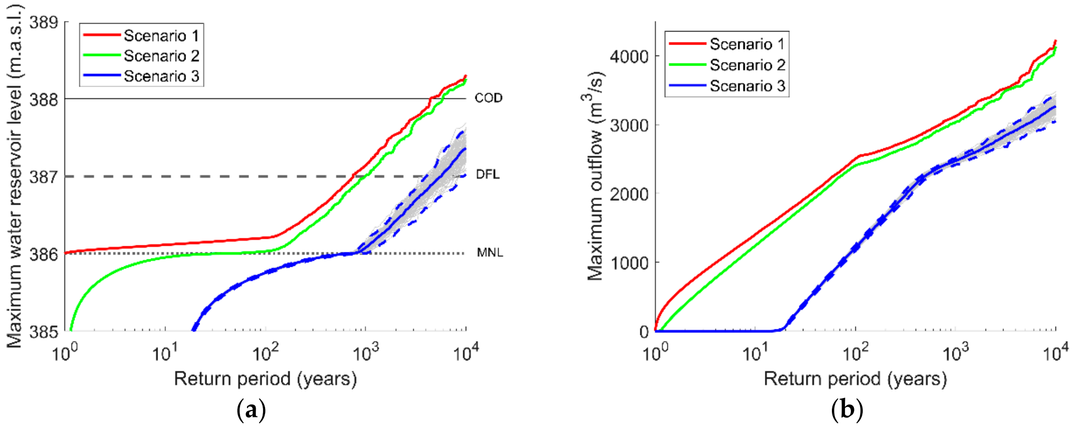

Figure 4. Maximum water reservoir level (MWRL) and maximum outflow (MO) frequency curves. (**a**) Red line represents the MWRL frequency curve assuming the initial level equal to Maximum Normal Level (MNL) (Scenario 1). Green line represents the MWRL frequency curve assuming the initial reservoir level equal to Flood Control Level (FCL) (Scenario 2). Grey lines represent the 1000 MWRL frequency curves, assuming the variable initial level (Scenario 3), being the median of these simulations represented by a blue continuous line and the 2.5% and 97.5% percentiles, with blue dashed-lines. The dotted grey line represents MNL, dashed grey line represents the Design Flood Level (DFL), continuous grey line represents the COD. (**b**) Same as figure (**a**) but applied to Maximum Outflow.

The most adverse situation regarding the hydrological dam and downstream safety was Sc. 1 (Figure 4). DFL was reached at a return period of 751 years, with an initial reservoir level of 386 m.a.s.l. Setting FCL at 384 m.a.s.l. (Sc. 2), the DFL was reached at a return period of 1000 years. In Sc. 3, the DFL was reached by the median MWRL frequency curve at 5647 years, whereas the 1000 frequency curves reached the DFL between 3710 and 9470 years. Overtopping occurred at 4427 and 5840 years in Scenario 1 and 2, respectively, whereas no overtopping occurred up to a 10,000 years of return period in Scenario 3.

When analyzing the MO frequency curves, the maximum capacity at MNL (2428 m^3/s) was reached at a return period of 87 years in Sc. 1, 111 years in Sc. 2, and 831 years for the median of the 1000 frequency curves. The 1000 frequency curves reached 2428 m^3/s between 709 and 1092 years.

In order to evaluate how the initial reservoir level affected the hydrological dam and downstream safety in terms of return period, we calculated an indicator proposed by Gabriel–Martin et al. [16], to analyze how the initial variable level affected the hydrological dam and downstream safety. This indicator represented the return period which corresponded to the same MWRL or MO that had a return period of 1000 years if MNL was assumed to be the initial reservoir level (Sc. 1), represented as Tr_{VAR}. In the case study, for the median MWRL frequency curve, $Tr_{VAR.}$ was equal to 7063 years, whereas for the MO frequency curve, $Tr_{VAR.}$ was equal to 7064 years. This behavior was similar to the ones obtained in previous studies, in which this indicator went from 3200 to 9000 years [14–16], for reservoirs whose main purpose was irrigation.

It should be highlighted that, if uncertainty due to the initial reservoir level is evaluated, the variation of this indicator could be seen. $Tr_{VAR.}$ ranged from a minimum of 4902 years to a maximum of 12,320 years, being the same minimum and maximum value in the case study of both MWRLs and MOs. This procedure is helpful to have an order of magnitude of how the initial reservoir level can influence the hydrological dam and downstream safety, but uncertainty should be accounted for, for more detailed results.

To analyze the uncertainty associated with the initial reservoir level, we carried out an analysis similar to the one proposed by Flores et al. [31]. We analyzed the different values associated with a given return period of MWRL (Table 2; represented as the height water above the Flood Control Level (m) for the sake of clarity) and MO (Table 3), obtaining the 25% percentile (Q1), the 50% percentile (Q2 or median), and the 75% percentile (Q3) quartiles. Moreover, in order to quantify the uncertainty of the estimations, the interquartile range (IQR) was calculated. The IQR is the difference between the upper and lower quartiles and permits the measurement of statistical dispersion.

Table 2. Values of the first (Q1), second (Q2), third (Q3) quartiles, the interquartile range (IQR), and the relative value of the IQR, against Q2, for different return periods (Tr) of maximum water reservoir levels. Values are represented as the water height above the Flood Control Level.

Tr (years)	Q1 (m)	Q2 (m)	Q3 (m)	IQR (m)	IQR/Q2 (%)
100	1.748	1.753	1.757	0.009	0.5
1000	2.050	2.075	2.093	0.043	2.1
5000	2.865	2.925	2.989	0.123	4.2
10,000	3.222	3.340	3.424	0.202	6.0

Table 3. Values of the first (Q1), second (Q2), third (Q3) quartiles, the interquartile range IQR, and the relative value of the IQR against Q2, for different return periods (Tr) of maximum outflows.

Tr (years)	Q1 (m^3/s)	Q2 (m^3/s)	Q3 (m^3/s)	IQR (m^3/s)	IQR/Q2 (%)
100	1200.3	1212.8	1222.8	22.5	1.9
1000	2455.8	2472.5	2483.3	27.5	1.1
5000	2949.5	2986.4	3025.4	76.0	2.5
10,000	3174.6	3250.1	3303.6	129	4.0

It can be seen how the uncertainty increased considerably, after a return period of 1000 years (Figure 4 and Table 2; Table 3). This behavior can be related to the configuration of spillway studied. Gated-spillway dams are designed with a maximum outflow capacity. When the outflow capacity corresponding to the MNL is reached, the VEM is not able to maintain the target reservoir level by operating the gates, the gates open, and floods cannot be controlled, which results into more variability. Furthermore, this variability is possibly related to the size of the sample of synthetic inflow hydrographs used (100,000), as shown by other authors, when studying stochastic approaches for deriving flood frequency curves [19–22]. We found out that the effect of the initial reservoir level on the MWRL and MO frequency curves have a small uncertainty (IQR/Q2 < 2.1%) for return periods below 1000 years, by using a 100,000 inflow hydrographs and 100,000 initial reservoir levels.

3.4. Risk Index Analysis

Finally, we quantified the influence of the initial reservoir variability in dam and downstream safety, by applying the global risk index procedure [18]. To do so, we obtained damage cost curves D_{MWRL} (Figure 5a) and D_{MO} (Figure 5b). By applying the procedure explained in the methodology, we were able to obtain the I_F, I_{NF}, and I_R, for the different scenarios. Figure 5c presents the values I_F, I_{NF}, and I_R associated with Sc. 1 and Sc. 2, and the median values of the 1000 simulations of Sc. 3. With regards to the different risk index values, we obtained the following results:

- Failure risk index (I_F): In the case of Sc. 1, I_F had a value of 526.4 $\times$ 10^3 euros, whereas in Sc. 2 I_F reduced to 242.6 $\times$ 10^3 euros. Regarding Sc. 3, the median value of I_F in the 1000 simulations was 85.2 $\times$ 10^3 euros, with values ranging from 77.6 $\times$ 10^3 euros to 99.0 $\times$ 10^3 euros (minimum and maximum value respectively). Therefore, I_F reduced its value by 83.8% from Sc. 1 to Sc. 3, and 64.8% from Sc. 2 to Sc. 1.

- Non failure risk index (I_{NF}): In the case of Sc. 1, I_{NF} had a value of 1442.6 $\times$ 10^3 euros, whereas in Sc. 2, I_{NF} reduced to 978.1 $\times$ 10^3 euros. Regarding Sc. 3, the median value of I_{NF} in the 1000 simulations was 89.8 $\times$ 10^3 euros, with values ranging from 83.6 $\times$ 10^3 euros to 94.0 $\times$ 10^3 euros (minimum and maximum value, respectively). Therefore, I_{NF} reduced its value by 94% from Sc. 1 to Sc. 3, and 91% from Sc. 2 to Sc. 1.
- Global risk index (I_R): In the case of Sc. 1, I_R had a value of 1968.9 $\times$ 10^3 euros, whereas in Sc. 2 I_R was reduced to 1220.7 $\times$ 10^3 euros. Regarding Sc. 3, the median value of I_R in the 1000 simulations was 175.1 $\times$ 10^3 euros, with values ranging from 163.7 $\times$ 10^3 euros to 191.6 $\times$ 10^3 euros (minimum and maximum value respectively). Therefore, I_R reduced its value by 91% from Sc. 1 to Sc. 3, and 86% from Sc. 2 to Sc. 1.

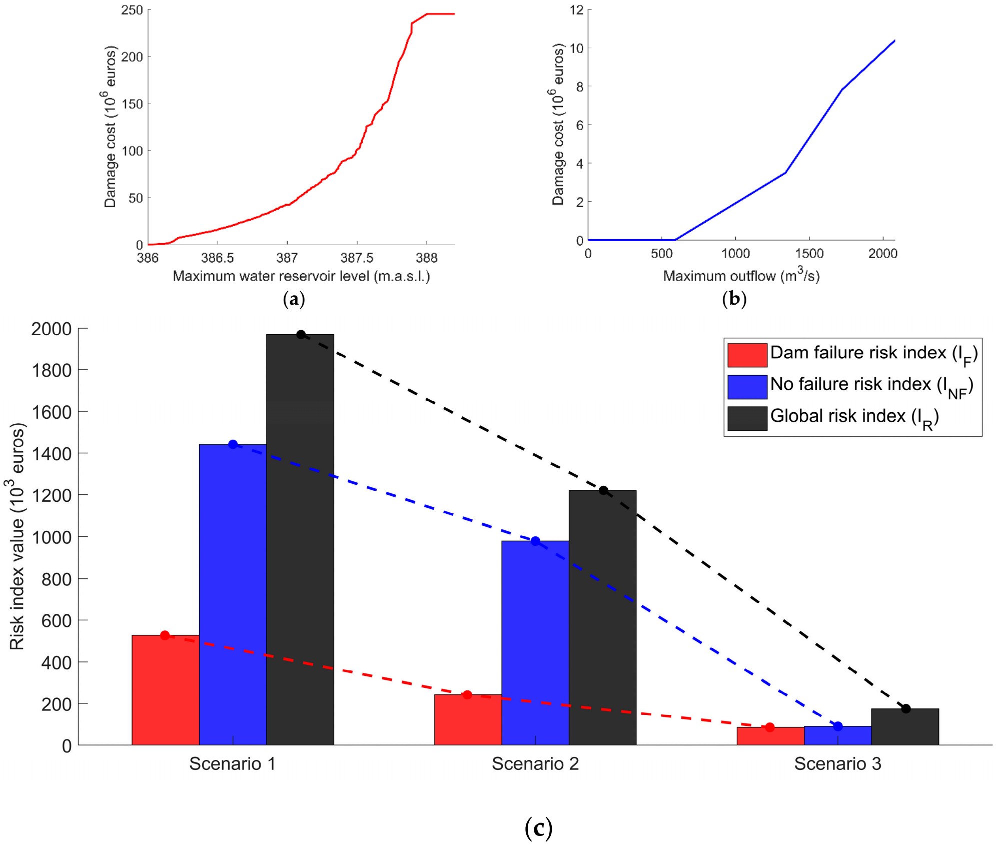

Figure 5. Damage cost curves. (**a**) Damage cost curves associated with maximum water reservoir levels. (**b**) Damage cost curves associated with maximum outflows. (**c**) Values of dam failure (I_F, red bars), non-failure (I_{NF}, blue bars), and global (I_R, black bars) risk index, for each of the three scenarios. Colored lines are added for a better comparison between the scenarios and the risk indices.

We quantified the uncertainty related to I_F, I_{NF}, and I_R with a similar procedure as the one discussed in Section 3.3, shown in Table 4. There is an uncertainty of 6.6%, 3.2%, and 4.2% associated with I_F, I_{NF}, and I_R, respectively, regarding the initial reservoir level. The value of uncertainty of I_F was higher than the uncertainty associated with I_{NF}. When evaluating I_F, the MWRLs values that had more importance for the risk index were those related to the extreme return periods (as can be seen in Figure 5a, there was no risk of damage below MNL). Therefore, the part of the MWRL frequency curve (Figure 4a) which was affected by the index in Sc. 3, was the one related to return periods over 1000 years, in which the uncertainty increased (Table 2). However, when evaluating I_{NF}, it could be seen that the damage (Figure 4b) started for values which correspond to medium return periods in Sc. 3 (from 40 years of the return period (Figure 4b)). As these values had less uncertainty (Table 3) and a higher value of exceedance probability (Figure 4b) than those affecting the I_F (Figure 4a and

Table 2), uncertainty was higher in I_F than I_{NF}, being the uncertainty of I_R between both values (as a consequence of Equation (2)).

Table 4. Values of the minimum, maximum, first (Q1), second (Q2), third (Q3) quartiles, the interquartile range (IQR), and the relative value of the IQR against Q2, for the dam failure (I_F), non-failure (I_{NF}), and the global (I_R) risk index.

Risk Index	Minimum (10^3 €)	Maximum (10^3 €)	Q1 (10^3 €)	Q2 (10^3 €)	Q3 (10^3 €)	IQR (10^3 €)	IQR/Q2 (%)
I_F	77.6	99.0	82.5	85.2	88.2	5.6	6.6
I_{NF}	83.6	94.0	88.3	89.8	91.1	2.8	3.2
I_R	163.7	191.6	171.2	175.1	178.6	7.4	4.2

It is important to point out that we did not consider the other aspects that might have an impact on the risk index analysis, such as the probability of failure due to blockage or malfunction of gates [16]. This would have resulted in higher values of MWRLs, for lower return periods [16], thus, resulting in higher values of I_{NF}, for all scenarios. Furthermore, this analysis could be complemented with studies of human loss of life, with societal risk indices [2,5], for a full comprehensive risk analysis.

4. Conclusions

The proposed methodology permitted the assessment of the influence of the initial reservoir level, the uncertainty related to this variable, and its influence in economic risk indices, through a stochastic procedure. The results obtained showed that:

- For the case study, considering that the fluctuation of the initial reservoir level provided a more realistic assessment of a hydrological dam and downstream safety. When a conventional approach was used (initial reservoir level equal to Maximum Normal Level), the Design Flood Level was reached at a return period of 751 years, which, therefore, did not fulfill the regulation standards (1000 years). However, when the initial reservoir level was accounted for, the results showed that the Design Flood Level was not reached in any of the set of 100,000 simulations carried out. When analyzing a portfolio of different reservoirs, a dam that might seem safer than others, at first, might not be so, if this variable was included in the analysis (for example, in an extreme case, comparing a hydroelectric dam—which is usually full—with a flood control reservoir—which is usually empty). Thus, this methodology can help stakeholders when carrying out decisions about prioritizing their investments.
- The influence of initial variable reservoir level on the maximum reservoir water level and maximum outflows frequency curves, observed in this case study, was within the range of other case studies conducted in previous research works [14–16]. In this case study, the return period considering the variable of initial reservoir for the value corresponding 1000 years, assuming initial reservoir level equal to MNL, was 7063 and 7064 years for the maximum reservoir water level and maximum outflow frequency curve, respectively.
- For the case study, we found out that the effect of the initial reservoir level on the maximum reservoir water level, and the maximum outflow frequency curve had a small uncertainty (less than 2.1%) for return periods below 1000 years, by using 100,000 inflow hydrographs and 100,000 initial reservoir levels.
- Within the case study, the global risk index reduced its value by 91% (if the variable initial reservoir level was accounted for) from 1968.9×10^3 (initial reservoir level equal to maximum normal level) to a median value of 175.1×10^3 euros (variable initial reservoir level).
- The uncertainty associated with the initial reservoir level fluctuation when calculating the global risk index was 4.2% (values ranging from 163.7 to 191.6 thousands of euros).

The proposed methodology was applied to one case study and dam configuration. Thus, extrapolation of results requires further work and applications to different case studies. Further research can be focused on the following topics:

- In order to account for the continuous variability in the natural processes and reservoir levels, a continuous modeling approach can be proposed. Thus, generation of stochastic weather forcing [32], coupled with a continuous hydrological model [33] can characterize, with a more accurate method, the seasonality of flood events (and therefore, is helpful for the definition of seasonal flood control levels). Furthermore, coupling the continuous hydrological forcing model with reservoir operations policies, permits the assessment of the impact of prior events on the initial reservoir levels, immediately before the maximum annual flood, providing a more reliable procedure to assess the effect of the initial reservoir level on dam safety.
- Within a continuous modeling framework, the impact of climate change on risk analysis can be assessed. For instance, stochastic weather generators can be perturbed, in order to assess the impact of climate change in flood events [32]. Additionally, future modifications in land use can be considered on the model framework [34], which, combined with population growth and changes in reservoir operation policies, can affect the complete cycle of dam risk assessment [2].
- Uncertainty associated with dam and downstream safety due to initial reservoir level might be assessed in other case studies, in order to propose simple indicators for dam risk assessment, in a way similar to Fluixá-Sanmartín et al. [35].
- By simulating the operation of the reservoir, initial reservoir level distributions can be obtained from the current operation of the reservoir, instead of from historical records [16,17]. By using the meteorological seasonal predictions and streamflow forecasts of the current year [36,37], a forecast distribution of the initial reservoir levels can be obtained and used as input for the dam risk model.
- Finally, influence of the initial reservoir level on the definition of flood control levels [17] can be economically assessed with a similar approach as the one presented in this paper. Thus, optimal flood control levels could be defined by combining an economic risk index related to water demand supply reliability [38], with the global risk index presented, herein, related to dam and downstream river safety.

Author Contributions: Conceptualization, Data curation, Formal analysis, Funding acquisition, Investigation, Methodology, Resources, Software, Validation, Visualization, Writing—Review & Editing, I.G.-M., A.S.-W., L.G. and I.G.; Supervision, A.S.-W., L.G. and I.G.; Writing—original draft, I.G.-M.

Acknowledgments: The authors would like to thank the funds from Fundación José Entrecanales Ibarra in the framework of the Program "Support program for research purposes". The authors acknowledge the computer resources and technical assistance provided by the Centro de Supercomputación y Visualización de Madrid (CeSViMa) and the funds from Universidad Politécnica de Madrid in the framework of "Programa propio: Ayudas para contratos predoctorales para la realización del doctorado en sus escuelas, facultad, centro e institutos de I+D+i", "Programa propio: ayudas a proyectos de I+D de investigadores posdoctorales", and "Consejo Social: XVI Convocatoria de ayudas del consejo social para el fomento de la formación y la internacionalización de doctorandos".

Conflicts of Interest: The authors declare no conflict of interest.

Abbreviations

The following abbreviations are used in this manuscript (sorted alphabetically).

A	Area of the watershed in km^2
ARMA	Autoregressive moving average model
COD	Crest of dam
$Cost_{break}$	Damage cost if the dam fails
D	Damage function
DFL	Design Flood Control Level
D_{MO}	Damage function associated to Maximum Outflows
D_{MWRL}	Damage function associated to Maximum Water Reservoir Levels

EAD	Expected annual damage
FCL	Flood Control Level
GEV	Generalized Extreme Value function
I_F	Failure risk index
IMF	Instantaneous maximum flow
I_{NF}	Non failure risk index
IQR	Interquartile range
I_R	Global risk index
L-MOM	L-Moments technique
m.a.s.l	Meters above sea level
MDF	Maximum annual mean daily flow
MNL	Maximum Normal Level
MO	Maximum Outflows
MWRL	Maximum Water Reservoir Level
$MWRL_{TR=1000y}$	Maximum Water Reservoir Level that corresponds to a return period of 1000 years
p	Probability of exceedance
$p(break \mid MWRL_i)$	Probability of overtopping failure conditioned to reaching a certain level in the reservoir
$p(MWRL_{MAX} \geq COD \mid MWRL_i)$	Probability of reaching the reservoir level at crest of dam once a certain reservoir level has been reached during a flood event
PFFC	Peak flow frequency curve
Q1	First quartile (25% percentile)
Q2	Median
Q3	Third quartile (75% percentile)
Sc. 1	Scenario in which initial reservoir level was set equal to Maximum Normal Level
Sc. 2	Scenario in which initial reservoir level was set equal to Flood Control Level
Sc. 3	Scenario in which initial reservoir level was considered variable
Tr	Return period
$Tr_{VAR.}$	Return period in Scenario 3 which corresponds to the same variable value of return period 1000 years in Scenario 1
VEM	Volumetric Evaluation Method
VFC	Volume frequency curve
Zo	Initial reservoir level prior to a flood event

References

1. Ren, M.; He, X.; Kan, G.; Wang, F.; Zhang, H.; Li, H.; Cao, D.; Wang, H.; Sun, D.; Jiang, X.; et al. A Comparison of Flood Control Standards for Reservoir Engineering for Different Countries. *Water* **2017**, *9*, 152. [CrossRef]
2. Fluixá-Sanmartín, J.; Altarejos-García, L.; Morales-Torres, A.; Escuder-Bueno, I. Review article: Climate change impacts on dam safety. *Nat. Hazards Earth Syst. Sci.* **2018**, *18*, 2471–2488. [CrossRef]
3. Australian National Committee on Large Dams (ANCOLD). *Guidelines on Risk Assessment*; Tech. rep.; Australian National Committee on Large Dams: Hobart, Australia, 2003.
4. United States Army Corps of Engineers (USACE). *Safety of Dams—Policy and Procedures*; Tech. Rep. ER 1110-2-1156; U.S. Army Corps of Engineers: Washington, DC, USA, 2011.
5. Spanish National Committe on Large Dams (SPANCOLD). *Risk Analysis as Applied to Dam Safety, Technical Guide on Operation of Dams and Reservoirs*; Professional Association of Civil Engineers: Madrid, Spain, 2012; Available online: http://www.spancold.es/Archivos/Monograph_Risk_Analysis.pdf (accessed on 24 October 2018).
6. Sordo-Ward, A.; Gabriel-Martin, I.; Bianucci, P.; Garrote, L. A Parametric Flood Control Method for Dams with Gate-Controlled Spillways. *Water* **2017**, *9*, 237. [CrossRef]
7. Sordo-Ward, A.; Bianucci, P.; Garrote, L.; Granados, A. How Safe is Hydrologic Infrastructure Design? Analysis of Factors Affecting Extreme Flood Estimation. *J. Hydrol. Eng.* **2014**, *19*, 12. [CrossRef]
8. Bianucci, P.; Sordo-Ward, A.; Moralo, J.; Garrote, L. Probabilistic-Multiobjective Comparison of User-Defined Operating Rules. Case Study: Hydropower Dam in Spain. *Water* **2015**, *7*, 956–974. [CrossRef]

9. Alemu, E.T.; Palmer, R.N.; Polebitski, A.; Meaker, B. Decision support system for optimizing reservoir operations using ensemble streamflow predictions. *J. Water Resour. Plan. Manag.* **2011**, *137*, 72–82. [CrossRef]
10. Labadie, J.W. Optimal operation of multireservoir systems: State-of-the-art review. *J. Water Resour. Plan. Manag.* **2004**, *130*, 93–111. [CrossRef]
11. Lund, J.R. Floodplain planning with risk-based optimization. *J. Water Resour. Plan. Manag.* **2002**, *128*, 202–207. [CrossRef]
12. Jain, S.K.; Yoganarasimhan, G.N.; Seth, S.M. A risk-based approach for flood-control operation of a multipurpose reservoir. *Water Resour. Bull.* **1992**, *28*, 1037–1043. [CrossRef]
13. Zeimetz, F.; Schaefli, B.; Artigue, G.; García Hernández, J.; Schleiss, A.J. New approach to identifying critical initial conditions for extreme flood simulations in a semicontinuous simulation framework. *J. Hydrol. Eng.* **2018**, *23*, 04018031. [CrossRef]
14. Carvajal, C.; Peyras, L.; Arnaud, P.; Boissier, D.; Royet, P. Probabilistic modelling of floodwater level for dam reservoirs. *J. Hydrol. Eng.* **2009**, *14*, 223–232. [CrossRef]
15. Aranda Domingo, J.A. Estimación de la Probabilidad de Sobrevertido y Caudales Máximos Aguas Abajo de Presas de Embalse. Ph.D. Thesis, Technical University of Valencia, Valencia, Spain, 2014. (In Spanish) [CrossRef]
16. Gabriel-Martin, I.; Sordo-Ward, A.; Garrote, L.; Castillo, L.G. Influence of initial reservoir level and gate failure in dam safety analysis. Stochastic approach. *J. Hydrol.* **2017**, *550*, 669–684. [CrossRef]
17. Gabriel-Martin, I.; Sordo-Ward, A.; Garrote, L. Influence of initial reservoir level on the allocation of seasonal maximum conservation levels. *Ing. Del Agua* **2018**, *22*, 225–238. [CrossRef]
18. Bianucci, P.; Sordo-Ward, A.; Perez, J.I.; Garcia-Palacios, J.; Mediero, L.; Garrote, L. Risk-based methodology for parameter calibration of a reservoir flood control model. *Nat. Hazards Earth Syst. Sci.* **2013**, *13*, 965–981. [CrossRef]
19. Loukas, A.; Quick, M.C.; Russell, S.O. A physically based stochastic-deterministic procedure for the estimation of flood frequency. *Water Resour. Manag.* **1996**, *10*, 415–437. [CrossRef]
20. Loukas, A. Flood frequency estimation by a derived distribution procedure. *J. Hydrol.* **2002**, *255*, 69–89. [CrossRef]
21. Blazkova, S.; Beven, K. Flood frequency estimation by continuous simulation of subcatchment rainfalls and discharges with the aim of improving dam safety assessment in a large basin in the Czech Republic. *J. Hydrol.* **2004**, *292*, 153–172. [CrossRef]
22. Sordo-Ward, A.; Garrote, L.; Martin-Carrasco, F.; Bejarano, M.D. Extreme flood abatement in large dams with fixed-crest spillways. *J. Hydrol.* **2012**, *466*, 60–72. [CrossRef]
23. USDA Soil Conservation Service (SCS). *National Engineering Handbook, Section 4: Hydrology*; USA Department of Agriculture: Washington, DC, USA, 1972.
24. Girón, F. The evacuation of floods during the operation of reservoirs. In *Transactions Sixteenth International Congress on Large Dams*; Report 75; International Commission on Large Dams (ICOLD): San Francisco, CA, USA, 1988; Volume 4, pp. 1261–1283.
25. Sordo-Ward, A.; Garrote, L.; Bejarano, M.D.; Castillo, L.G. Extreme flood abatement in large dams with gate-controlled spillways. *J. Hydrol.* **2013**, *498*, 113–123. [CrossRef]
26. Arnell, N.W. Expected annual damages and uncertainties in flood frequency estimation. *J. Water Resour. Plan. Manag.* **1989**, *115*, 94–107. [CrossRef]
27. Ministerio de Medio Ambiente y Medio Rural y Marino (MARM). *Guía Metodológica para el Desarrollo del Sistema Nacional de Cartografía de Zonas Inundables*; Secretaría General Técnica del Ministerio de Medio Ambiente y Medio Rural y Marino: Madrid, Spain, 2011.
28. Escuder-Bueno, I.; González-Pérez, J. *Metodología para la Evaluación del Riesgo Hidrológico de Presas y Priorización de Medidas Correctoras*; Colegio de Ingeniero de Caminos, Canales y Puertos: Madrid, Spain, 2014.
29. Hosking, J.R.M. L-moments: Analysis and estimation of distributions using linear combinations of order statistics. *J. R. Stat. Soc.* **1990**, *52*, 105–124. [CrossRef]
30. Gringorten, I.I. A plotting rule for extreme probability paper. *J. Geophys. Res.* **1963**, *68*, 813. [CrossRef]
31. Flores-Montoya, I.; Sordo-Ward, Á.; Mediero, L.; Garrote, L. Fully Stochastic Distributed Methodology for Multivariate Flood Frequency Analysis. *Water* **2016**, *8*, 225. [CrossRef]
32. Fatichi, S.; Ivanov, V.Y.; Caporali, E. Simulation of future climate scenarios with a weather generator. *Adv. Water Resour.* **2011**, *34*, 448–467. [CrossRef]

33. Vivoni, E.R.; Mascaro, G.; Mniszewski, S.; Fasel, P.; Springer, E.P.; Ivanov, V.Y.; Bras, R.L. Real-world hydrologic assessment of a fully-distributed hydrological model in a parallel computing environment. *J. Hydrol.* **2011**, *409*, 483–496. [CrossRef]
34. Pumo, D.; Arnone, E.; Francipane, A.; Caracciolo, D.; Noto, L.V. Potential implications of climate change and urbanization on watershed hydrology. *J. Hydrol.* **2017**, *554*, 80–99. [CrossRef]
35. Fluixá-Sanmartín, J.; Altarejos-García, L.; Morales-Torres, A.; Escuder-Bueno, I. Review article: Empirical Tool for the Assessment of Annual Overtopping Probabilities of Dams. *J. Water Res. Plan.* **2018**, *145*, 04018083. [CrossRef]
36. Delgado-Ramos, F.; Hervás-Gámez, C. Simple and Low-Cost Procedure for Monthly and Yearly Streamflow Forecasts during the Current Hydrological Year. *Water* **2018**, *10*, 1038. [CrossRef]
37. Tayyab, M.; Ahmad, I.; Sun, N.; Zhou, J.; Dong, X. Application of Integrated Artificial Neural Networks Based on Decomposition Methods to Predict Streamflow at Upper Indus Basin, Pakistan. *Atmosphere* **2018**, *9*, 494. [CrossRef]
38. Solera-Solera, A.; Morales-Torres, A.; Serrano-Lombillo, A. Cost estimation of freeboard requirements in water resources management. In *Risk Analysis, Dam Safety, Dam Security and Critical Infrastructure Management*; CRC Press: London, UK, 2012; pp. 9–14. [CrossRef]